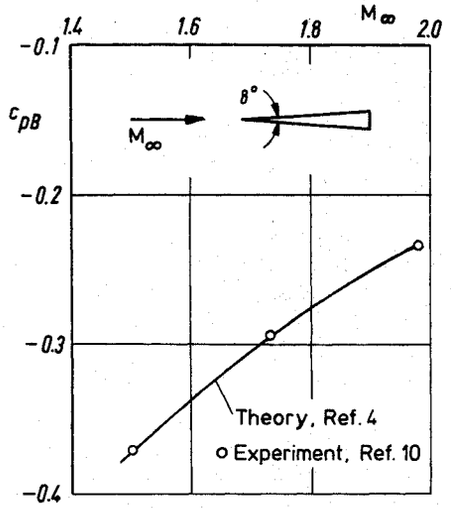

Fig. 4 Base pressure coefficient as a function of the Mach number (theory from Tanner,[4] experimental results from Tanner[10]).

For incompressible flow, the value $\delta_2/d=0.040$ was obtained by methods given by Schlichting[6] with the ratio δ_2/d as defined by Eqs. (21.8) and (21.9) in Ref. 6. As stated in Ref. 6, the boundary-layer thickness δ increases rapidly with increasing Mach number. Since, simultaneously, the ratio δ_2/d becomes smaller, it seems plausible to assume that δ_2/d increases only moderately with increasing Mach number. For our calculations, $\delta_2/d=0.045$ was used, which is 12.5% greater than the value $\delta_2/d=0.040$ valid for incompressible flow.

The experimental base pressure coefficients for the 30-deg wedge are smaller than for the extended ogive. In both cases, the use of a thick wire ($d=10$ mm) in front of the leading edge of the model causes a remarkable increase of the base pressure. This is an influence of the boundary-layer thickness because the base pressure increases with increasing boundary-layer thickness, as already shown in Ref. 1.

In Fig. 3, c_{pB} is plotted as a function of the freestream Mach number. The theoretical curves calculated by equations given in Ref. 4 agree very well with experimental values of the base pressure coefficient. For the 10-deg wedge, the wind-tunnel experiments of Ref. 9 agree well with the theoretical curve, whereas the C_{pB} values obtained in free flight are considerably lower, except at $M_\infty=6$, where theory and experiment agree. For the 30-deg wedge, the theoretical C_{pB} values are for the Mach number $M_\infty>4.6$, somewhat lower than vacuum. The theoretical base pressure is therefore negative, which is absurd. The reason for this anomaly is, at present, obscure. For $M_\infty\leq 4.0$, theoretical and experimental base pressure coefficients obtained for the 30-deg wedge are in good agreement, however.

In Fig. 4, results are shown for the 8-deg wedge in the Mach number range $M_\infty=1.5$–2.0. In this case, the agreement between theory and experiment is excellent.

Conclusions

Magi and Gai[2] claim that the value $H^*/H=7.37$ as used by the present author is valid only at low supersonic Mach numbers and that H^*/H should decrease with increasing Mach number. In their opinion, the value of H^*/H should be of the order of unity for Mach numbers $M_\infty>3.5$ (see Fig. 2 of Ref. 2).

The new results presented here in Figs. 1–4 show, however, that using the value $H^*/H=7.37$ at all Mach numbers gives theoretical results, which agree very well with experimentally observed base pressure coefficients for Mach numbers up to $M_\infty=7$. Therefore, the value $H^*/H=7.37$ seems to be universally applicable, contrary to the claims of Magi and Gai.[2]

References

[1]Tanner, M., "Boundary Layer Thickness and Base Pressure," *AIAA Journal*, Vol. 23, No. 12, 1985, pp. 1987–1989.

[2]Magi, E. C., and Gai, S. L., "Supersonic Base Pressure and Lip-shock," *AIAA Journal*, Vol. 26, No. 3, 1988, pp. 370–372.

[3]Nash, J. F., "A Discussion of Two-Dimensional Turbulent Base Flows," ARC R&M, 3468, July 1965.

[4]Tanner, M., "Steady Base Flows," *Progress in Aerospace Sciences*, Vol. 21, No. 2, 1984, pp. 81–157.

[5]Tanner, M., "Basisdruckmessungen an einer Platte und an einem Keil in dem Machzahlbereich von $Ma=2,8$ bis 6,8," *Zeitschrift für Flugwissenschaften*, Vol. 20, No. 11, 1972, pp. 410–413.

[6]Schlichting, H., *Boundary Layer Theory*, 7th ed., McGraw-Hill, New York, 1979.

[7]Matting, F. W., Chapman, D. R., Nyholm, J. R., and Thomas, A. G., "Turbulent Skin Friction at High Mach Numbers and Reynolds Numbers in Air and Helium," NASA TR R-82, 1961.

[8]Saltzman, E. J., "Base Pressure Coefficients Obtained From the X-15 Airplane for Mach Numbers up to 6," NASA TN D-2420, Aug. 1964.

[9]Hopkins, E. J., Fetterman, D. E., and Saltzman, E. J., "Comparison of Full-Scale Lift and Drag Characteristics of the X-15 Airplane with Wind-Tunnel Results and Theory," NASA TM X-713, 1962.

[10]Tanner, M., "Druckverteilungsmessungen an Keilen bei kompressibler Strömung, *Zeitschrift für Flugwissenschaften*, Vol. 18, No. 6, 1970, pp. 202–208.

Numerical Investigation of Unsteady Transonic Nozzle Flows

Shen-Min Liang* and Chou-Jiu Tsai†
National Cheng Kung University, Tainan, Taiwan, Republic of China
and
Chien-Ko Ho‡
Chung Shan Institute of Science and Technology, Lungtan, Taiwan, Republic of China

Introduction

UNSTEADY flow phenomena have frequently occurred in many places during aircraft flight such as flutter on wings caused by the interaction of elastic, inertial, and aerodynamic forces, buffeting at airfoil trailing edge due to strong shock/boundary-layer interaction, and buzz in inlets. The avoidance of these unwanted, unsteady flow phenomena through understanding their flow structures would be beneficial for aircraft design.

In this study, unsteady transonic nozzle flows with shock waves are considered, resulting from a fluctuating backpressure. In the past, unsteady nozzle flows with shocks has been studied by several investigators.[1-4] In Ref. 1, Richey and Adamson found that in the slowly time-varying regime, the amplitude of shock oscillation is $\mathcal{O}(\epsilon)$ if the imposed pressure fluctuation has an amplitude of $\mathcal{O}(\epsilon^2)$ and period of order ϵ^{-1}, where ϵ denotes a small parameter used to measure the difference between the flow velocity and the sound speed. Thus, the shock oscillation is linearly related to the imposed pressure fluctuation. In their study, the wall thickness was assumed to be $\mathcal{O}(\epsilon^2)$. However, in the present study it is found that the wall

Received July 29, 1990; revision received Dec. 11, 1990; accepted for publication Dec. 17, 1990.

*Associate Professor, Institute of Aeronautics and Astronautics. Member AIAA.

†Graduate Student, Institute of Aeronautics and Astronautics.

‡Assistant Scientist.

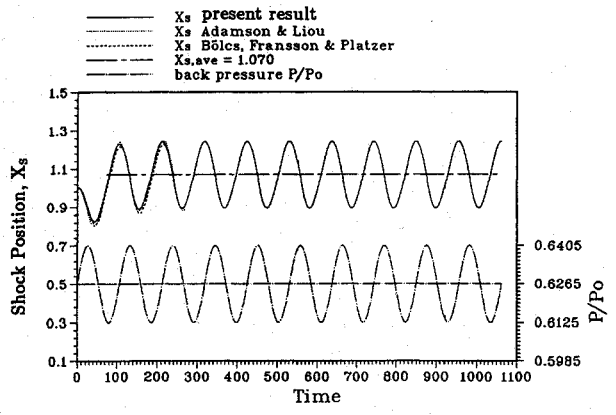

Fig. 1 Comparison of computed shock position with existing results ($\bar{P} = 0.014$; $K = 0.059$).

thickness is also an important parameter that can cause linear relations not to exist for larger values of wall thickness.

An alternative to asymptotic techniques that need the assumption of a sufficiently small parameter is numerical simulation. The numerical simulation is prospective, since fast and large-memory digital computers are currently available. Numerical methods used to analyze unsteady channel flows with shocks has been done by several researchers.[5,6] In Ref. 5, the mass-averaged Navier-Stokes equations with k-ω turbulence model was solved by using MacCormack's hybrid method that is time-consuming. In Ref. 6, Bölcs et al. employed the flux-splitting approach, leading to the use of upwind schemes, to solve the time-dependent Euler equations. Their results are reasonably accurate compared to existing results, except for some slight oscillations occurring near the shock.

In addition to the parameter of wall thickness, two other important parameters involving the unsteady nozzle flow are the fluctuating amplitude and frequency of the pressure. The extent of the influence of these three parameters on the shock movement is explored in this study. To accurately capture the shock at any instant, a time-accurate, high-resolution, total variation diminishing (TVD) scheme[7-9] is constructed. To enhance convergence rate, the alternating direction implicit (ADI) form of Beam and Warming[10] is used. A numerical example used in the paper of Bölcs et al.[6] is computed for comparison. Relations between the changes both in amplitude and frequency of the fluctuating pressure and the shock oscillation are investigated.

Contents

Mathematical Formulation

Assume that the nozzle flow is inviscid and compressible, and that there is no external force present. The equations governing the flow are the Euler equations.[6] Presume that the flow is a perfect gas with constant ratio of specific heats γ. The pressure is related by other variables:

$$p = (\gamma - 1)[e - \tfrac{1}{2}\rho(u^2 + v^2)] \tag{1}$$

where p is the pressure, ρ the density, u,v the Cartesian velocity components, and e the total energy per unit volume.

Numerical Procedure

Time-Accurate Implicit TVD Schemes

To admit weak solutions, the Euler equations are discretized in a finite-volume fashion. Since the flow variables are evaluated at the volume interfaces, the Roe average for density evaluation at volume interfaces is adapted.[11] The TVD scheme introduced by Yee and Harten[7] is employed. To efficiently solve the difference equations, the approximate factorization form of Beam and Warming[10] is used.

Choice of Time Step

Implicit schemes allow use of a larger time step unlike explicit schemes that have the stability limitation of the Courant number *CFL* being less than unity. For achieving a fast convergence, a spatially varying time step is used. Using these characteristic times, the time step is set to be the Courant number times the minimum of the characteristic times over the whole flow domain.

Boundary Conditions

In this study, only one- and quasi-one-dimensional nozzle flows are considered. The boundary conditions needed to be imposed are at the inlet and the outlet. The number of boundary conditions at the entrance or at the exit depends on the number of characteristics that the wave propagates into the flow domain. In the present study, the flow both at the entrance and at the exit is subsonic. Two boundary conditons of constant entropy and constant $R = u_\infty + 2a_\infty/(\gamma - 1)$, a Riemann invariant, are prescribed at the entrance, and one boundary condition of imposed pressure (based on the entrance total pressure) is imposed at the exit. Other flow variables at the entrance or at the exit are calculated by the characteristic equation(s) through iteration.

Results and Discussion

To verify the accuracy of the present method both in time and space, the shock-tube problem is solved first. Steady and unsteady channel flows with shock waves are calculated next. Numerical results were performed on the Alliant FX-80 computer.

Shock-Tube Problem

In this problem a uniform grid with 200 cells is selected on a flow domain. The Courant number *CFL* is chosen to be 1 for a fast convergence. It was found that the computed result is in good agreement with the exact solution.[12] Because of the space limitation, the result is not shown. This shows that the present time-accurate scheme is able to accurately predict time-dependent solutions.

Quasi-One-Dimensional Nozzle Flows

Case 1: Smooth Wall with Continuous Curvature

For comparison of the present solution, the quasi-one-dimensional nozzle flow studied by Adamson and Liou,[4] also studied by Bölcs et al.,[6] is calculated. The nozzle has the following cross-sectional area distribution:

$$A(x) = 1 + \epsilon^2 f(x) \tag{2}$$

where $f(x)$ is given in Ref. 4. A uniform grid with 120 cells is used. In order to obtain a steady-state solution, a larger value of *CFL*, $CFL = 30$, is chosen to accelerate the convergence process. With the computed steady-state flow, the back-pressure is perturbed by a sinusoidal wave:

$$P_b = 0.6265 + \bar{P}\sin[K(t - t_0)] \tag{3}$$

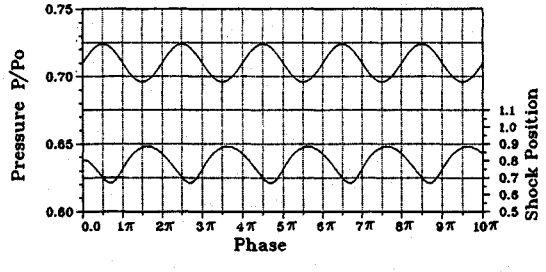

Fig. 2 Shock oscillation in response to imposed pressure fluctuation in nozzle with a 10% circular-arc shape throat.

Only small values of K are considered for practical applications in jet engines.[4] For $\bar{P} = 0.014$, $K = 0.059$, and $\epsilon = 0.1$, the flowfield and the shock movement caused by the backpressure fluctuation have been reported in detail by Bölcs et al.[6] In this study, the unsteady flow is computed for many cycles of pressure fluctuation and *CFL* is set at 1.5. Figure 1 shows periodic oscillations of the shock position as time advances. Existing results are included in the figure for comparison. It is shown that the present result is closer to the analytic solution of Adamson and Liou than that obtained by Bölcs et al. It was found that there is a 90-deg phase lag in shock oscillation. Moreover, the shock-oscillation frequency is the same as the frequency of imposed pressure fluctuation, and the imposed pressure fluctuation linearly affects the shock movement.[12]

Case 2: 1% and 10% Circular-Arc Throats

Now consider a nozzle with a 1% circular-arc shape throat. Note that the nozzle wall has a discontinuous curvature at the wall junctures. Thus, the analytic method used by Richey and Adamson fails to apply. However, the present numerical method does not have such a limitation. It was found that similar results of linear relations and a 90-deg phase lag as presented in case 1 were obtained. We will see the results in Figs. 3 and 4.

When the circular-arc thickness is changed from 1 to 10%, the previous linear relations may not exist. Figure 2 shows the shock oscillation as the backpressure fluctuates. Because of larger disturbances produced by the thicker wall, the phase lag is increased from 90 to 158 deg. That means that the wall thickness plays an important role. The thicker the wall, the more the phase lag.

Figure 3 shows the change quantities ($\Delta X_{s,\text{amp}}$, $\Delta X_{s,\text{av}}$) of amplitude and average position of shock oscillation for 1% and 10% circular-arc throats, respectively, as the frequency of imposed shock oscillation is varied. For the 1% case, the pressure-fluctuation frequency is varied from 0.005 to 0.015 at fixed amplitude $\bar{P} = 0.001$. For the 10% case, the pressure-fluctuation frequency is varied from 0.05 to 0.3 at fixed amplitude $\bar{P} = 0.0195$. Note that $K = 0.005$ is chosen as a reference point (origin of coordinate) for the 1% case, and $K = 0.1$ for the 10% case. In the present calculations, the chosen values of the parameters K and $\bar{P}$ are varied about their reference points so that the normal shock does not move across the throat into the subsonic region. It is seen that for the 10% case, the shock-oscillation amplitude is nonlinearly decreased and the average shock position is nonlinearly increased as the frequency of imposed pressure fluctuation is increased.

Figure 4 shows the change in quantities of amplitude and average position of shock oscillation for 1% and 10% circular-arc throats, respectively, as the amplitude of imposed pressure fluctuation is varied. Note that the frequency of imposed pressure fluctuation is fixed at $K = 0.035$ and the pressure fluctuation amplitude is varied from 0.0005 to 0.0045 for the

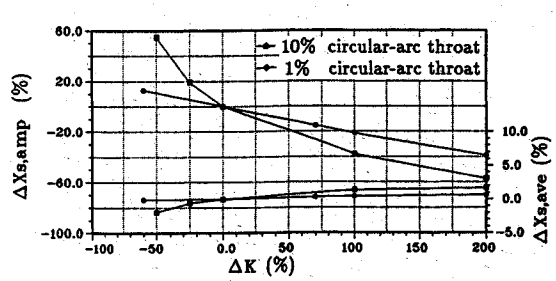

Fig. 3 Variations of shock-oscillation amplitude and average shock position with change quantity in frequency of imposed pressure fluctuation ($P = 0.0195$).

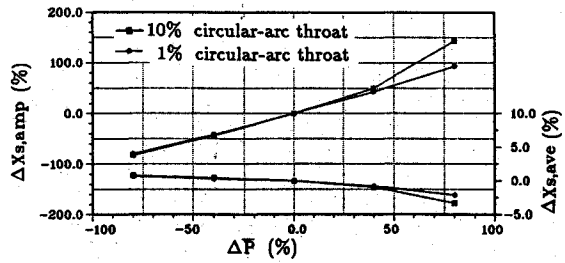

Fig. 4 Variations of shock-oscillation amplitude and average shock position with change quantity in amplitude of imposed pressure fluctuation ($K = 0.0035$).

1% case and from 0.002 to 0.018 for the 10% case. The reference points are set to $\bar{P} = 0.0025$ for the 1% case and $\bar{P} = 0.01$ for the 10% case. For the 1% case, linear relations exist only when $\bar{P} \leq 0.0035$. When $\bar{P} > 0.0035$, the data start to deviate from the linear curves. Larger deviations are found to occur for the thicker throat. This means that the shock-oscillation frequency is not the same as the frequency of imposed pressure fluctuation. It is found that the average shock position can be greater than 3% for larger values of $\bar{P}$ (>0.0035).

Acknowledgment

The support for this study, under the contract of the National Science Council of the Republic of China, NSC-79-0401-E-006-38, is gratefully acknowledged.

References

[1]Richey, G. K., and Adamson, T. C., Jr., "Analysis of Unsteady Transonic Channel Flow with Shock Waves," *AIAA Journal,* Vol. 14, No. 8, 1976, pp. 1054–1061.

[2]Adamson, T. C. Jr., Messiter, A. F., and Liou, M. S., "Large Amplitude Shock-Wave Motion in Two-Dimensional Transonic Channels," *AIAA Journal,* Vol. 16, No. 12, 1978, pp. 1240–1247.

[3]Culick, F. E. C., and Rogers, T., "The Response of Normal Shocks in Diffusers," *AIAA Journal,* Vol. 21, No. 10, 1983, pp. 1382–1390.

[4]Adamson, T. C., Jr., and Liou, M. S., "Unsteady Motion of Shock Waves in Two-Dimensional Transonic Channel Flows," Dept. of Aerospace Engineering, Univ. of Michigan, Rept. UM-014534-F, Ann Arbor, MI, June 1977.

[5]Liou, M. S., and Coakley, T. J., "Numerical Simulation of Unsteady Transonic Flow in Diffusers," *AIAA Journal,* Vol. 22, No. 8, 1984, pp. 1139–1145.

[6]Bölcs, A., Fransson, T. H., and Platzer, M. F., "Numerical Simulation of Inviscid Transonic Flow Through Nozzles with Fluctuating Back Pressure," *ASME Journal of Turbomachinery,* Vol. 111, April 1989, pp. 169–180.

[7]Yee, H. C., and Harten, A., "Implicit TVD Schemes for Hyperbolic Conservation Laws in Curvilinear Coordinates," *AIAA Journal,* Vol. 25, No. 2, 1987, pp. 266–274.

[8]Yee, H. C., "A Class of High-Resolution Explicit and Implicit Shock-Capturing Methods," NASA TM-101088, Feb. 1989.

[9]Yee, H. C., "Linearized Form of Implicit TVD Schemes for the Multidimensional Euler and Navier-Stokes Equations," *Computers and Mathematics with Applications,* Vol. 12A, No. 4/5, 1985, pp. 413–432.

[10]Beam, R. M., and Warming, R. F., "An Implicit Factored Scheme for the Compressible Navier-Stokes Equations," *AIAA Journal,* Vol. 16, No. 4, 1978, pp. 393–402.

[11]Roe, P. L., "Approximate Riemann Solvers, Parameter Vectors, and Difference Schemes," *Journal of Computational Physics,* Vol. 43, No. 2, 1981, pp. 357–372.

[12]Liang, S. M., and Ho, C. K., "Numerical Investigation of Unsteady Transonic Nozzle Flows Using Time-Accurate TVD Schemes," *Proceedings of the 7th National Conference of the Chinese Society of Mechanical Engineering,* Vol. 1, Hsingchu, Taiwan, ROC, Nov. 1990, pp. 669–676.